EasyChair Preprint

№ 8221

Towards Autonomous Robotic Ultrasound Scanning Using Pneumatically Attachable Flexible Rails

Aoife McDonald-Bowyer, Solene Dietsch,
Emmanouil Dimitrakakis, Joanna Coote, Lukas Lindenroth,
Danail Stoyanov and Agostino Stilli

EasyChair preprints are intended for rapid dissemination of research results and are integrated with the rest of EasyChair.

June 10, 2022

Towards Autonomous Robotic Ultrasound Scanning using Pneumatically Attachable Flexible Rails

A. McDonald-Bowyer[1], S. Dietsch[1], E. Dimitrakakis[1], J. Coote[1], L. Lindenroth[1], D. Stoyanov[1], and A. Stilli[1]

[1] *Wellcome/EPSRC Centre for Interventional and Surgical Sciences (WEISS)*
a.mcdonald-bowyer.19@ucl.ac.uk

INTRODUCTION

Robotic-assisted partial nephrectomy (RAPN) is a surgical procedure that employs robotics to remove a portion of diseased kidney. During the procedure, a drop-in Ultrasound (US) probe is used to identify the resection margins. Although the robot facilitates the task, the scanning of the kidney proves challenging due to slippage and requires a highly skilled surgeon [1]. In previous work [2], we presented a Pneumatically Attachable Flexible (PAF) rail to enable stable, track-guided US scanning of the kidney during RAPN. In [3] and [4], we have investigated the autonomous deployment of the PAF rail on the surface of the organ and their use in intraoperative organ manipulation. In [5], Wang et al. studied the 3-D reconstruction of a mass embedded in a kidney phantom when the PAF rail guides the US probe. In this work, we investigate autonomous control during the US scanning using the PAF rails, specifically using fibre-optic shape-sensing data as the input for path-planning. First, we present the design and fabrication of the sensorized PAF rail; then we assess the performance of real-time curvature sensing with the sensorized PAF rail system on rigid and soft phantoms; finally, we demonstrate how the PAF rail local shape data can be used to plan a trajectory and autonomously guide an intraoperative US probe.

MATERIALS AND METHODS

Design and Fabrication of Sensorized PAF Rail - We updated the design of the PAF rail based on the optimisation design study firstly presented in [2] and later in [5]. We incorporated a 1 mm channel along its internal perimeter to embed fine bore low-density polyethylene (LDPE) tubing (0.86 mm ID, 1.52 mm OD), which houses a multi-core shape sensing fibre (FBGS International, Jena, Germany). Each core contains 25 FBGs spaced at 10 mm intervals. The PAF rail was manufactured using injection moulding of DragonSkin™30 silicone (Smooth-On, Macungie, PA, US).

Design and Fabrication of Phantoms - We laser cut seven concentric ($R = 30, 50, 70, 90, 110$ mm) grooves (see Fig. 1a) into a sheet of acrylic plastic to evaluate the curvature sensing performance of the bare fibre. Phantoms of the same curvature range were fabricated in

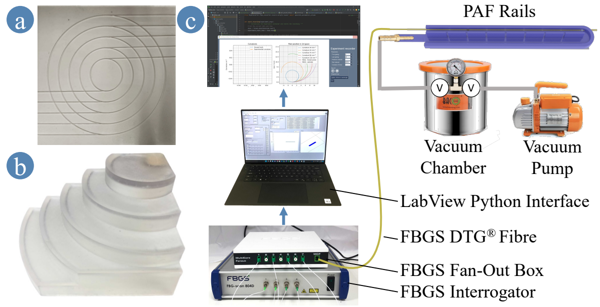

Fig. 1 a) Acrylic laser-cut plate. b) Rigid curvature block. c) Hardware schematic: The shape-sensing fibre is thread through the fine-bore tubing and fixed at the distal end with Sil-Poxy Silicone adhesive. The rail is then attached to a 12-litre vacuum chamber via a barb connector and tubing, which is vacuumized by a 3 CFM single-stage vacuum pump. The fibre is connected to an optical interrogator via a multi-core fibre fan-out.

rigid plastic (see Fig. 1b), hard silicone rubber (Smooth-On, DragonSkin™30) and soft silicone rubber (Smooth-On, EcoFlex™00-20). These materials were chosen to reflect the large range of mechanical properties of kidney tissue reported in the literature [6] [7]. Finally, we created a negative mould from segmented CT images to fabricate a geometrically realistic kidney phantom. We cast tissue-mimicking material (polyvinyl alcohol - PVA) following the procedure in [8] and included a spherical structure of stiffer PVA to replicate a mass.

Curvature Sensing - First, we examined the curvature sensing performance of the bare shape-sensing fibre to set the ground truth comparison. We recorded and averaged the curvature over 30 iterations after threading the fibre along each groove of the acrylic plate. Then, we embedded the fiber in the PAF rails. A pneumatic circuit was set up as shown in Fig. 1c. The PAF rail was suctioned to each surface of the rigid curvature block and soft curvature phantoms while we recorded the sensed curvature for 5 seconds. *Autonomous Ultrasound Scanning* - As a proof-of-concept, we automated the track-guided US scan using the first generation da Vinci surgical robot [9] and the sensorized PAF rails. We equipped the first da Vinci Patient Side Manipulator (PSM1) with the EndoWrist® Prograsp™ Forceps paired with the drop-in US probe BK X12C4 (BK-Medical Holding Inc., Peabody, Massachusetts), as shown in Fig. 2. The PAF rail is suctioned to the kidney

TABLE I DS30 Sensed Curvature Errors

R (mm)	Max ϵ ($\times 10^{-2} mm^{-1}$)	(%)	Mean ϵ ($\times 10^{-2} mm^{-1}$)	(%)
30	2.64 ± 0.91	8.80	5.68 ± 0.25	18.9
50	1.6 ± 0.89	3.20	3.51 ± 0.25	7.02
70	0.57 ± 1.15	0.81	2.38 ± 0.33	3.40
90	0.39 ± 1.11	0.43	1.82 ± 0.34	2.02
110	0.11 ± 0.95	0.10	1.49 ± 0.28	1.35

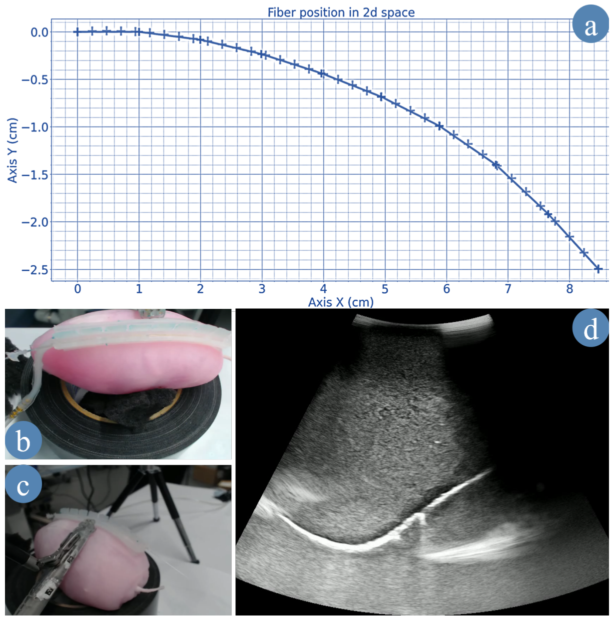

Fig. 2 Feasibility study snapshot. a) Computed drop-in US trajectory. b) Camera top view. c) Camera lateral view. d) Stream snapshot recorded with the drop-in US probe.

phantom while the PSM1/US probe pair is manually positioned perpendicular to the first fibre grating. A snapshot of the sensed fibre shape is taken, converted to a trajectory and relayed to the dVRK to control the PSM1 using the Robot Operating System (ROS). It executes a scan of the phantom, delivering a real-time US stream.

RESULTS

The average sensing error of the bare FBGS fibre is 1.02 ± 0.03 (2.9%) (Fig. 3). When embedded in the rail and tested on the rigid phantoms, the average sensing error increases to 6.5%. Sensing accuracy deteriorates with smaller radius of curvature, from 1.25% at $R = 110$ mm to 18.9% at $R = 30$ mm (see Table I). The trajectory

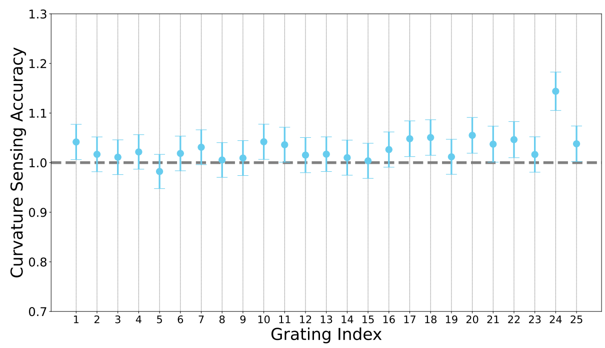

Fig. 3 Curvature sensing accuracy at each grating position along the fibre. Accuracy is defined as the ratio of sensed curvature to geometric curvature. For perfect sensing, we would expect a value of 1 for each grating.

for PSM1 was successfully obtained from the sensorized rail (Fig. 2d) and the trajectory was executed by PSM1. The probe maintained contact with the rail for 20 mm and an US stream was obtained (Fig. 2a).

DISCUSSION

We autonomously guided an ultrasound probe during the scan of a kidney phantom from the sensed curvature of the PAF rails. Here, we present promising results but, further study is needed to improve the US trajectory accuracy as we made several assumptions. Namely, curvature uniformity along the width of the rail, we manually positioned the probe perpendicular to the rail to reduce the problem from 3-D to 2-D planning, and we did not account for the offset between the US probe and the PSM1 tip.

As expected, we experienced larger curvature sensing errors of the sensorized PAF rails at tighter radii ($R = 30$ mm). However, in this context, the PAF rails are oriented along the long axis of the kidney. In this region, R ranges between 70 and 110 mm which corresponds to a sensing accuracy range of 1.35% - 3.4%. Or to a maximum position error of 0.024 mm and 1.16 mm for the full length of the rails. These results are satisfactory for path planning.

Overall, we demonstrate the applicability of shape sensing in soft robotics to automate an intraoperative robotic US scan. In a further study, we aim to perform multiple US swipe sequences to enhance the US scan quality and compare the robot performance against clinical standards. Another improvement would be to develop a calibration process to remove systematic errors when the rail is under suction.

REFERENCES

[1] C. G. Rogers *et al.*, "Robotic Partial Nephrectomy for Complex Renal Tumors: Surgical Technique," *European Urology*, vol. 53, no. 3, pp. 514–523, 3 2008.

[2] A. Stilli *et al.*, "Pneumatically Attachable Flexible Rails for Track-Guided Ultrasound Scanning in Robotic-Assisted Partial Nephrectomy A Preliminary Design Study," *IEEE ROBOTICS AND AUTOMATION LETTERS*, vol. 4, no. 2, 2019.

[3] C. D'Ettorre *et al.*, "Semi-Autonomous Interventional Manipulation using Pneumatically Attachable Flexible Rails," *IEEE International Conference on Intelligent Robots and Systems*, pp. 1347–1354, 11 2019.

[4] C. D'Ettorre *et al.*, "Autonomous pick-and-place using the dVRK," *International Journal of Computer Assisted Radiology and Surgery*, vol. 16, no. 7, p. 1141, 7 2021.

[5] C. Wang *et al.*, "Ultrasound 3D reconstruction of malignant masses in robotic-assisted partial nephrectomy using the PAF rail system: a comparison study," *International Journal of Computer Assisted Radiology and Surgery (2020).*, vol. 15, no. 7, pp. 1147–1155, 5 2020.

[6] F. Adams *et al.*, "Soft 3D-Printed Phantom of the Human Kidney with Collecting System," *Annals of Biomedical Engineering*, vol. 45, no. 4, pp. 963–972, 4 2017.

[7] C. L. Cheung *et al.*, "Use of 3-dimensional printing technology and silicone modeling in surgical simulation: development and face validation in pediatric laparoscopic pyeloplasty," *Journal of surgical education*, vol. 71, no. 5, pp. 762–767, 2014.

[8] E. C. Mackle *et al.*, "Wall-less vascular poly(vinyl) alcohol gel ultrasound imaging phantoms using 3D printed vessels," *https://doi.org/10.1117/12.2510033*, vol. 10870, pp. 66–72, 2 2019.

[9] "The da Vinci Research Kit (dVRK) – Intuitive Foundation." [Online]. Available: https://www.intuitive-foundation.org/dvrk/